International Forum on Aeroelasticity and Structural Dynamics
IFASD 2019
10-13 June 2019 Savannah, Georgia, USA

ERROR ESTIMATION AND POD-BASED REFERENCE SELECTION TO APPROXIMATE GAF MATRICES FOR FLUTTER

Hendrik Verdonck[1], **Reik Thormann**[1], **Hans Bleecke**[1], **Bernd Stickan**[1]

[1]Airbus Operations GmbH
Loads and Aeroelastics
Airbus-Allee 1, 28199 Bremen, Germany
hendrikverdonck@gmail.com and reik.thormann@airbus.com

Keywords: Flutter, LFD, POD, GAF approximation

Abstract: During flutter analyses of aircraft a large parameter space has to be analyzed covering not only the extended flight envelope but also a large set of mass variations and failure cases. The generalized aerodynamic forces are computed for a reference mass case applying a linearized frequency domain method based on the Reynolds-averaged Navier-Stokes equations. The aerodynamic matrices for different mass cases are approximated using a least-square approach. While this approach is working for most normal mass cases, larger deviations in flutter predictions can occur for discrete structural failures. Error criteria are developed to estimate if the approximation is within bounds without calculating the aerodynamic response of the actual modes. The modal assurance criterion is compared to a local error, weighting the modal displacements with their corresponding aerodynamic forces, as well as a norm of the generalized aerodynamic force matrices. The three error estimators are benchmarked for a discrete structural failure case showing a similar performance. Furthermore, if the maximal error exceeds a certain threshold, the reference basis used in least-square approach has to be augmented to improve the prediction. While a suitable residual mode can be found by engineering judgment, an automatic process is preferable. A proper orthogonal decomposition is applied to find the most dominant error mode. This approach can also be applied to define a better reference mode set directly in the beginning of the process. Instead of using the mode shapes of a reference mass case, the modes of several mass cases including failure cases are used as snapshots. Results are presented comparing frequency and damping progressions as function of speed for a transport aircraft at nominal and failure conditions.

1 INTRODUCTION

In flutter analysis, the stability of the coupled system of structural, aerodynamic and inertia forces has to be ensured for a parameter space to cover the extended flight envelope, spanned by e.g. flight altitude and Mach number. In addition, several mass variations and failure cases have to be analyzed. In the current process, generalized aerodynamic force (GAF) matrices are computed applying the linearized frequency domain (LFD) method [1–3]. The underlying nonlinear Reynolds-averaged Navier-Stokes (RANS) equations are linearized around a steady flow field, computed by a nonlinear, coupled fluid-structure simulation. The obtained linear system is transformed into the frequency domain resulting in a large, sparse system of linear equations. This approach maintains the dynamic characteristics of the underlying nonlinear RANS model. Although the LFD method is about two orders of magnitude faster than its

nonlinear counterpart, it is too expensive to directly compute all variations (and evolutions) of the structural model. Instead, a least-square approach (LSQA) is used to approximate the GAF matrices for different mass cases. A correlation matrix is computed relating the set of reference modes to the set of modes for the case of interest. Due to linearity, the same transfer matrix can be used to approximate the aerodynamic forces. The quality of this LSQA depends on the reference mode set. If the production modes are approximated well, the aerodynamic forces will be accurate. A typical choice is to select one mass case as reference to approximate all other cases. While this approach is expected to work properly for nominal mass cases, larger deviations in flutter predictions can occur for discrete structural failures. The structural dynamics of this case are not sufficiently resolved by the reference mode set and therefore the basis needs to be enhanced [4].

First, an error criterion is developed to estimate if the approximation is within bounds without calculating the aerodynamic response of the actual modes. The modal assurance criterion [5, 6] might not be sufficient, since local errors could be averaged out if there is a good agreement for a large number of structural nodes. Therefore, a local criterion is conducted evaluating the maximal error. Two additional estimators are analyzed: In the first, the error mode is weighted by the aerodynamic forces and thus, the maximal difference of the local work per mode is evaluated. In the second criterion, a relative GAF error is computed. Secondly, if the maximal error exceeds a certain threshold, the basis used in the LSQA has to be augmented to improve the prediction. While a suitable residual mode can be found by engineering judgment, an automatic process covering all mass and failure cases is preferable. A proper orthogonal decomposition (POD) is applied to find the most dominant error mode. POD is a modal decomposition technique which determines the optimal set of modes to represent a reference set based on the L_2 norm, which is commonly referred to as 'energy' of the input modes [7]. POD was introduced for aeronautical application by Lumley as a method to extract coherent structures from a turbulent flowfield [8, 9]. Moreover, it is actively researched as a method for model reduction in unsteady aerodynamic simulations [7, 10–12]. This approach can also be applied to define a better reference mode set directly in the beginning of the process. The input will be a set of vibration modes of the aircraft for different structural layouts and mass distributions. The aim of the POD method is thus to decompose this input mode set in an optimal, orthogonal reference set.

Results are presented to compare the three different error estimators for a transport aircraft. In addition, the two approaches to choose the reference basis are compared for nominal and failure cases. Frequency and damping progressions as function of equivalent airspeed are analyzed. Moreover, influence of different setups for the POD are discussed on basis of the introduced error criterion.

2 NUMERICAL METHOD

2.1 Flutter Simulation Process

The classical flutter simulation is a linear stability analysis examining if small perturbations of the system grow or decay in amplitude. Therefore, a linear structural model is used and transformed into generalized coordinates. Moreover, the aerodynamic forces can be linearized around a steady, mean state and projected onto the modal basis. Physically, the static, aeroelastic equilibrium, defining the point of linearization, depends on the dynamic pressure, too. However, this effect is neglected during these flutter analyses, which are computed for constant Mach number.

The governing unsteady aeroelastic equation in the frequency domain and in generalized coordinates reads

$$\left[\mathbf{M}^* p^2 + \mathbf{D}^* p + \mathbf{K}^* - \frac{\rho_\infty}{2} U_\infty^2 \mathbf{GAF}(M_\infty, p)\right] \hat{\mathbf{q}} = \mathbf{0},$$

with the Laplace variable p, free-stream velocity U_∞, density ρ_∞, Mach number M_∞, generalized coordinate vector $\hat{\mathbf{q}}$ and generalized mass, damping and stiffness matrices $\mathbf{M}^*$, $\mathbf{D}^*$ and $\mathbf{K}^*$, respectively. The generalized air force matrix can be computed as

$$\mathbf{GAF} = \frac{2}{\rho_\infty U_\infty^2} \mathbf{\Phi}^T \mathbf{F}_A(s) \mathbf{\Phi},$$

with the aerodynamic response of small perturbation $\mathbf{F}_A(s)$ and the eigenvector matrix $\mathbf{\Phi}$. The flutter boundary is computed by an in-house pk-solver [13], considering only the imaginary part of the Laplace variable when evaluating the GAF matrix. MSC-NASTRAN [14] is used to establish the dynamic structural matrices and to perform the modal analysis, whereas the DLR-TAU code [15] is applied to solve the RANS equations. FlowSimulator [16] is used as the data handling framework linking all computational aeroelastic modules and enabling fluid-structure interaction [17, 18]. Steady, coupled simulations are conducted to obtain the static elastic equilibrium for one flight level. Afterwards, the unsteady aerodynamics are computed applying (LFD) solver [1, 19] using the linearized Spalart-Allmaras turbulence model [20].

2.2 GAF Approximation

The unsteady aerodynamics are only computed for a set of reference elastic mode shapes. The results are mapped to different mass and structural layout cases using a least-squares approach based on the relative mode shapes of the production case and the reference case, respectively. The production modes are represented as a linear combination of the reference mode shapes and a correlation matrix $\mathbf{\Psi}$, with ϵ being the residual vector:

$$\mathbf{\Phi}_{\text{prod}} = \mathbf{\Phi}_{\text{ref}} \mathbf{\Psi} + \boldsymbol{\epsilon}.$$

The correlation matrix is found by minimizing the RMS of the residual using the pseudo-inverse

$$\mathbf{\Psi} = \left(\mathbf{\Phi}_{\text{ref}}^T \mathbf{\Phi}_{\text{ref}}\right)^{-1} \mathbf{\Phi}_{\text{ref}}^T \mathbf{\Phi}_{\text{prod}}.$$

The reference GAF matrix is then projected to the production case by

$$\text{GAF}_{\text{prod}} = \mathbf{\Psi}^T \text{GAF}_{\text{ref}} \mathbf{\Psi}.$$

Note that the goal of the approximation is to map the unsteady aerodynamic results. The modes in the LSQA should therefore represent as closely as possible the modes on the CFD surface which are seen by the flow solver. Assuming that the CFD surface nodes are evenly distributed over the surface suggests, that selecting the CFD surface points is a good starting point to represent these modes. The modes described on the structural grid have to be interpolated to the CFD surface nodes for each flutter computation to accomplish this. However, this is a computationally expensive process which is not practically feasible to be repeated for all flutter computations. The LSQA can therefore only be executed on the structural finite element nodes. The influence of different node selections was studied and a manual selection of structural nodes, as visualized in Figure 1, showed the best performance. All aircraft components have a considerable weight in the approximation and the mode shapes can be captured accurately in all desired degrees of freedom.

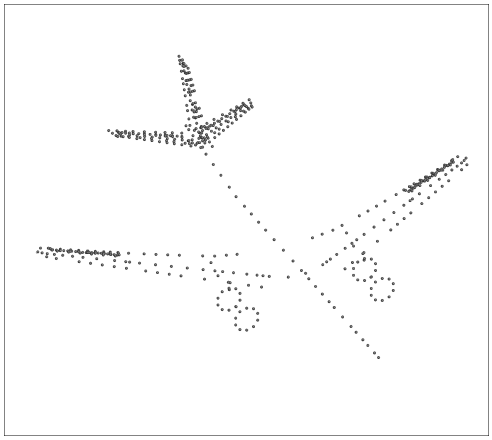

Figure 1: Manually selected node set for mode representation in LSQA

2.3 Proper Orthogonal Decomposition

POD is used to provide an objective algorithm to decompose an expanded mode set covering multiple mass and structural layout cases in a reference set. The input modes are structured in a matrix with as column dimension the number of considered modes and as row dimension the degrees of freedom of each of these modes. The implementation of the POD method depends on the size of the input matrix. If the column dimension exceeds the row dimension, which would be the case if a large set of reference cases and only a subset of the degrees of freedom of the FEM is used, the classical POD method should be applied. When the opposite is true, which could be the case if all nodes and degrees of freedom of the FEM are used or if only a small set of reference cases is considered, the method of snapshots should be applied. Both solution strategies are introduced here. Note that these methods give the same result, and the only reason for selecting one or the other is the memory and computational efficiency of the POD.

2.3.1 Classical POD method

Consider $\mathbf{X}$ to be the input matrix with m number of elastic mode shapes and n number of degrees of freedom. The POD modes will be the eigenvectors of the eigenvalue problem of dimension n:

$$\mathbf{X}\mathbf{X}^T\boldsymbol{\phi}_n = \lambda_n\boldsymbol{\phi}_n,$$

with $\boldsymbol{\phi}$ the resulting POD eigenvectors, which can be assembled in a POD eigenvector matrix $\boldsymbol{\Phi}$ and λ the eigenvalues corresponding to each of the POD modes.

2.3.2 Method of snapshots

As mentioned, if the row dimension is large, the size of matrix $\mathbf{R} = \mathbf{X}\mathbf{X}^T$ can pose memory or computational time issues. Instead, the method of snapshots computes the eigenvalue problem on the, in this case, much smaller matrix $\mathbf{X}^T\mathbf{X}$:

$$\mathbf{X}^T\mathbf{X}\boldsymbol{\theta}_m = \lambda_m\boldsymbol{\theta}_m.$$

The solution of this eigenvalue problem gives the same eigenvalues, but the POD eigenvector matrix $\boldsymbol{\Phi}$ has to be recovered from the computed eigenvectors $\boldsymbol{\theta}$ by

$$\boldsymbol{\Phi} = \mathbf{X}\boldsymbol{\Theta}\boldsymbol{\Lambda}^{-1/2}$$

with the input matrix $\mathbf{X}$, the intermediate eigenvector matrix $\boldsymbol{\Theta}$ and a diagonal matrix with the eigenvalues $\boldsymbol{\Lambda}$.

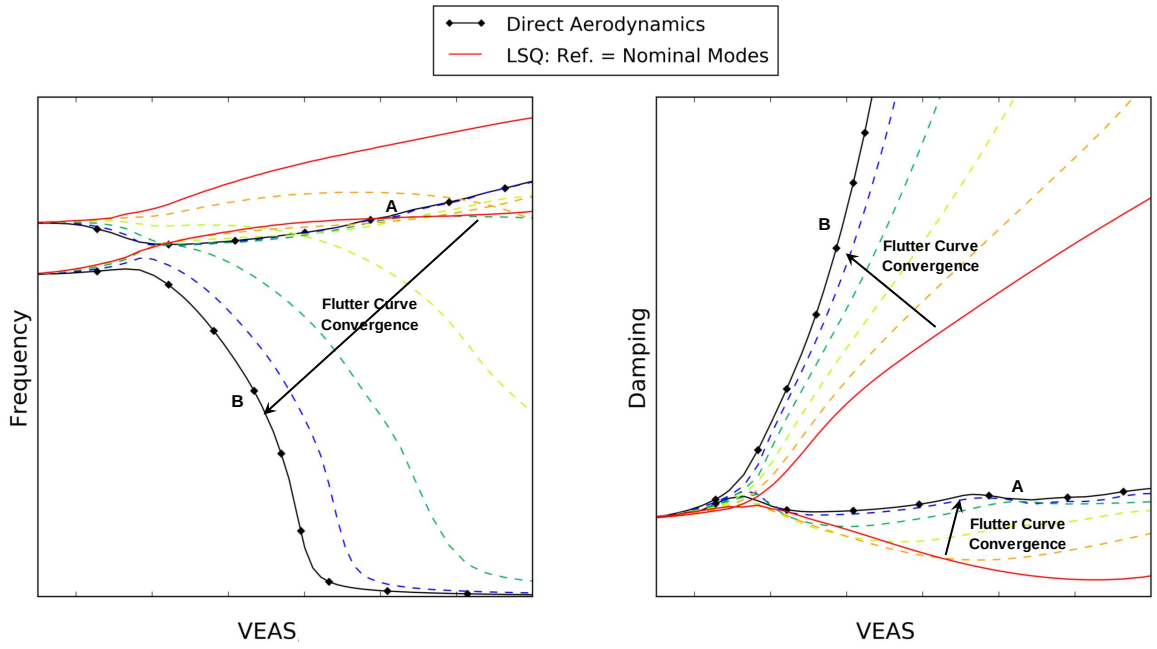

Figure 2: Flutter curve convergence by modifying the stiffness of the additional mode for the failure case

2.3.3 Properties of the POD mode set

The resulting set of POD modes has some useful properties. The POD modes are orthonormal and sorted by the relative information content they represent of the input modes. The strictly real and positive eigenvalue corresponding to each resulting mode is a measure for the amount of energy represented by that mode. Therefore, the eigenvalues are commonly used as truncation parameter to decide how many of the resulting modes should be used in order to capture approximately all energy contained in the reference. Only r number of POD modes have to be retained such that

$$\frac{\sum_{j=1}^{r} \lambda_j}{\sum_{j=1}^{n} \lambda_j} \approx 1,$$

with the eigenvalues λ and the total number or resulting POD modes n.

3 ERROR ESTIMATION

3.1 Test Case Description

The test case is based on a flutter computation of a generic aircraft model with a structural deficiency to create mode shapes which can locally strongly deviate from those with a nominal structure. The reference modal basis is made up out of nominal structure modes for the full considered frequency range enhanced with one mode accounting for the failure case to tune the model. The stiffness of this added mode is step-by-step reduced to have a smooth transition from the nominal structural model to the considered failure case. Figure 2 shows the frequency and damping progression for two modes of this test case. The direct aerodynamics approach serves as reference solution, directly computing the aerodynamic response to the production modes without the LSQA. These plots show a convergence of the flutter curves from the approximation with only nominal structure reference modes (solid, red line) to the verification result, while

reducing the stiffness of the additional reference mode. This gives a suitable test case for the error estimation study as the performance of the proposed quality criteria can be tested by linking them to each step of this convergence.

3.2 Quality Criteria

The error estimator should give a measure for the induced error of the LSQA on a production flutter computation for a given reference modal basis. Following criteria are applied in the comparison.

3.2.1 MAC Error

A commonly used metric to quantify the correlation between two modes is the MAC (mode assurance criterion). The MAC error quality criterion is computed as

$$\text{MAC Error} = 100\% \cdot \max \left\{ 1 - \frac{\left(\boldsymbol{\phi}_i^T \boldsymbol{\phi}_i'\right)^2}{\left(\boldsymbol{\phi}_i^T \boldsymbol{\phi}_i\right)\left(\boldsymbol{\phi}_i'^T \boldsymbol{\phi}_i'\right)} \right\}_{i=1,\ldots,n_{\text{modes}}},$$

with $\boldsymbol{\phi}$ the exact production modes, $\boldsymbol{\phi}' = \boldsymbol{\phi}_{\text{ref}}\boldsymbol{\Psi}$ the approximate production modes and n_{modes} the number of production modes. The MAC criterion is a standard tool in practice for modal correlation of theoretical models to experimental vibrational tests [5, 6]. However, the hypothesis was that this criterion could be insufficient to capture local mode errors, such as the one introduced by the test case. These local mode approximation errors could still have a large impact on the GAF matrix and consequently on the frequency and damping progression. Therefore two additional quality criteria are established.

3.2.2 Aerodynamic-Weighted Local Mode Approximation Error

This local mode error weights the local mode approximation error on each of the considered structural nodes by the magnitude of the unsteady aerodynamic forces and therefore is a measure for the error in the induced aerodynamic work. The quality criterion is normalized as

$$\text{Aero-Weighted Local Mode Approx. Error} = 100\% \cdot \max \left\{ \frac{\max\left(\boldsymbol{\epsilon}_{w,i}\right)}{\max\left(\boldsymbol{\phi}_{w,i}\right)} \right\}_{i=1,\ldots,n_{\text{modes}}}.$$

with $\boldsymbol{\epsilon}_w = \boldsymbol{\epsilon} \circ |\mathbf{F}_a'|$ the element-wise product of the least-square residual and the magnitude of the unsteady aerodynamic forces and $\boldsymbol{\Phi}_w = \boldsymbol{\Phi} \circ |\mathbf{F}_a'|$ the exact production modes weighted by aerodynamic forces. Note that the approximate aerodynamic forces $\mathbf{F}_a'$ have to be interpolated to the structural grid to enable the element-wise weighting.

3.2.3 Approximate GAF Error

As third criterion an approximate GAF error is computed as

$$\text{Relative GAF Error} = 100\% \cdot \max \left\{ \frac{|\mathbf{GAF}_{ii}^e|}{|\mathbf{GAF}_{ii}'|} \right\}_{i=1,\ldots,n_{\text{modes}}},$$

with $\mathbf{GAF}^e = \boldsymbol{\epsilon} \cdot |\mathbf{F}'_a|$ and $\mathbf{GAF}' = \boldsymbol{\Phi} \cdot |\mathbf{F}'_a|$ the approximate GAF error matrix and the approximate GAF matrix, computed by a matrix product with the magnitude of the unsteady aerodynamic forces. Only the diagonal elements on the approximate GAF matrices are considered, which describe the amount of energy added or subtracted to a certain mode by the unsteady aerodynamics of its own modal deformation.

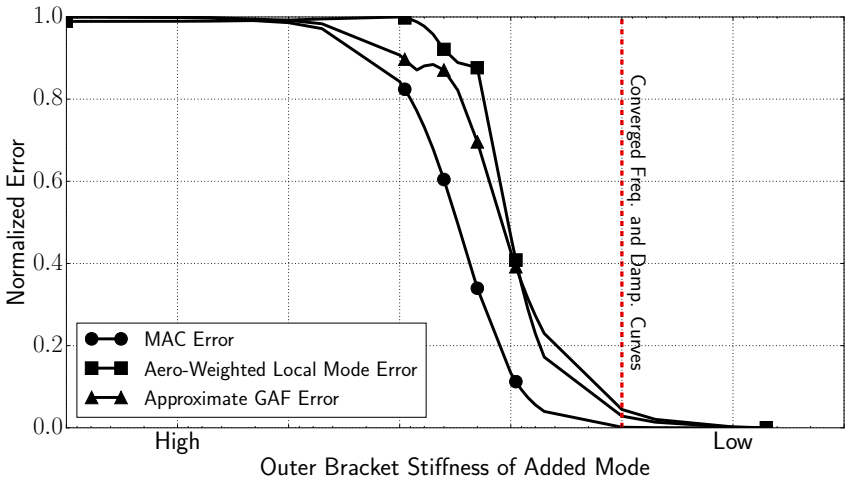

Figure 3: Convergence of proposed quality criteria

3.3 Results

The results for the three proposed quality criteria are shown in Figure 3. The markers on each line correspond to the intermediate convergence curves presented in Figure 2, whereas the lines are constructed out of 25 intermediate convergence steps. The red dotted line indicates the point where no longer a deviation between the approximation and the direct aerodynamics could be observed. The three proposed criteria show a clear convergence corresponding to the convergence in the frequency and damping progression. All three criteria are therefore good predictors of the influence of the mode approximation error on the frequency and damping progression. The hypothesis that the MAC would not be sufficient is therefore disproved for this test case scenario. While both other estimators show a larger gradient at the ”convergence-line”, the additional computational complexity does not justify the small benefit of a slightly clearer criterion.

Based on the results for this test case scenario, best-practice quality thresholds can be established for each criterion. For the MAC error criterion this was defined at 1%, which will be used in the upcoming sections.

3.4 Modal Basis Enrichment

When the error estimators indicate an insufficient reference set, enrichment of this modal basis is necessary. The test case showed that the addition of a single mode of the structurally deficient structure sufficed to eliminate the mode approximation error. This is caused by the similarity of the residual for all critical modes with respect to the approximation. The normalized residual for the three most critical modes is shown in Figure 4. These figures also show the highly local appearance of the mode approximation error around the location of the structural deficiency. The residual similarity implies that the introduced structural deficiency created a piece of orthogonal modal information which could not be reproduced by a linear combination of the

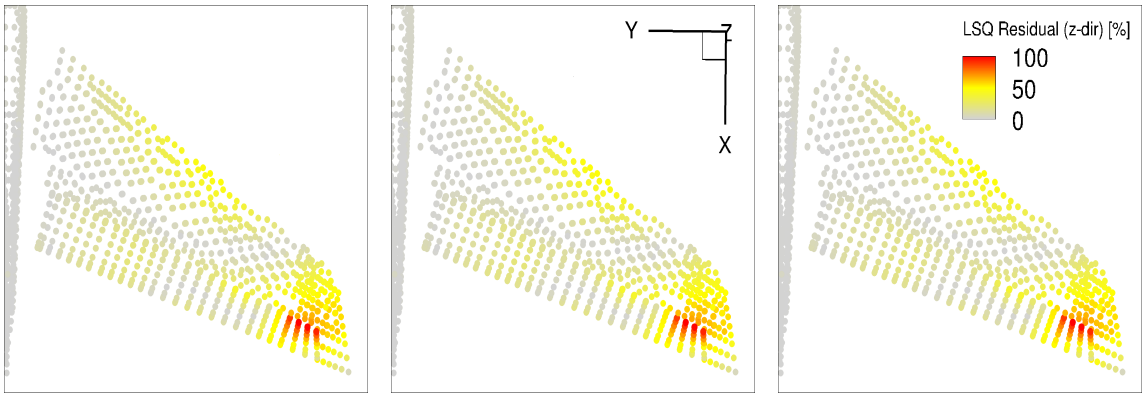

Figure 4: Max. normalized LSQA residual ϵ for the three most critical modes

nominal structure reference modes. The mode approximation error can therefore be solved by adding this piece of information to the reference set. This can be achieved by a basis enrichment with a critical production mode or the residual for one of these critical production modes. More advanced methods like finding the dominant residual through a POD analysis was - for this test case scenario - not required.

4 POD-BASED REFERENCE MODAL BASIS SELECTION

The error estimation study showed the importance of the reference modal basis. A new method is proposed to improve the reference modal basis selection. The POD theory is used to decompose an expanded modal basis spanning multiple structural layouts and mass distributions in a reference set. This should give more robust results for structural failure cases while retaining the approximation accuracy for nominal structure flutter computations. Results will be compared to a reference set containing only the nominal structure modes for one mass distribution. Both methods are verified by the direct aerodynamic results. The performance of the two reference selection methods will be tested by two test cases. The first one is a nominal structure flutter computation without any structural deficiencies, thus creating mode shapes which should be easy to approximate. Secondly, the structural failure case discused in the error estimation will be re-used.

4.1 POD-Based Reference Setup

The performance of the POD-based reference selection method is strongly influenced by its set-up. The first factor is the selection of the POD input cases. Which mass and structural layout cases are used as snapshots for the POD decomposition? For this test case scenario only the structural layouts of the test cases will be used as input. In total 7 different load cases with a nominal structural layout were used, alongside 3 load cases for each of the 2 considered failure cases.

For each combination of structural layout and mass distribution, a selection of the modes can be made. The effect of a frequency limit on the modes for a certain input case is visualized in Figure 5. These figures give the MAC error for all modes of one of the test cases sorted by their natural frequency. Four different frequency limits are imposed on the input case. This shows that a good approximation can only be achieved for those modes which lay inside the frequency band used for the POD snapshots. Imposing a frequency limit of 10Hz results in

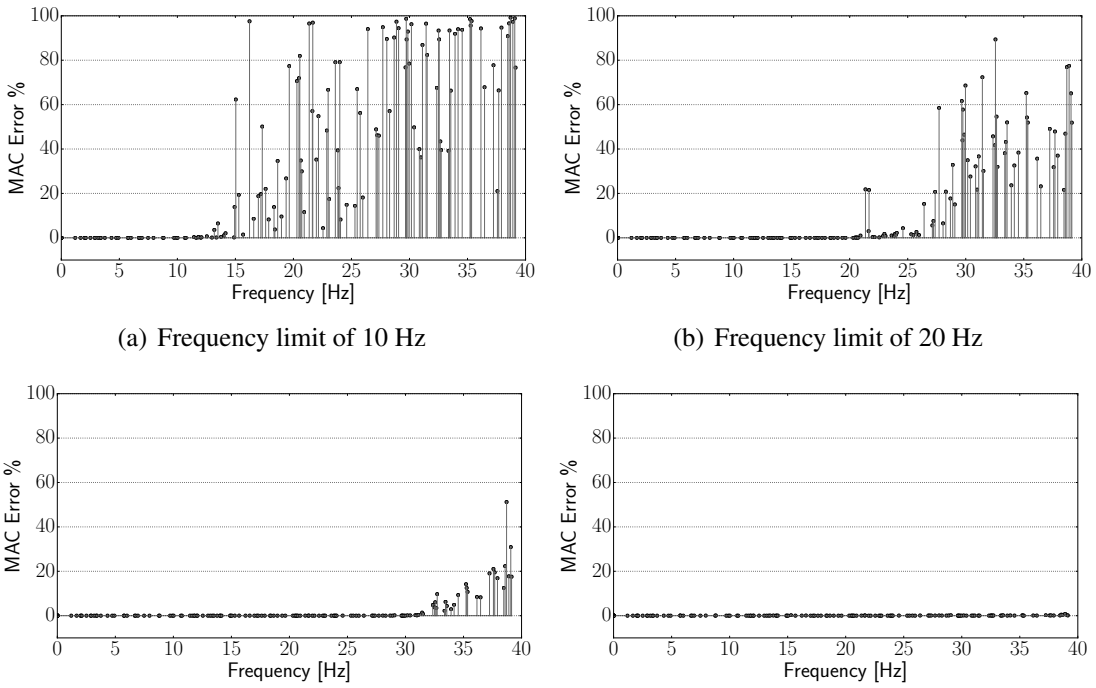

(a) Frequency limit of 10 Hz

(b) Frequency limit of 20 Hz

(c) Frequency limit of 30 Hz

(d) No frequency limit

Figure 5: Effect of an imposed frequency limit on the POD input modes on the MAC error for all modes of failure case

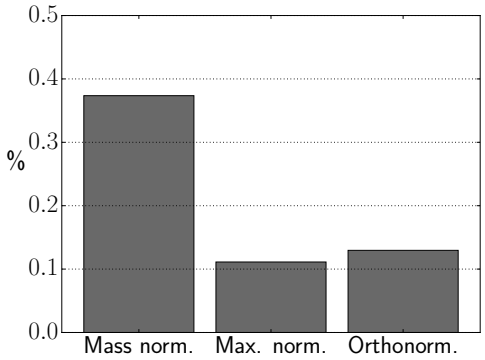

Figure 6: MAC error criterion for different normalizations

large approximation error for modes around $15Hz$. A similar result is obtained using a limit of 30Hz, while using a 20Hz limit already causes more than 20% MAC error at 21Hz. Modes with higher natural frequency exhibit more local deflections which cannot be represented by low-frequency modes.

The POD will decompose the input based on the L_2 norm of the input modes. The mode normalization therefore determines the error norm which is minimized by the POD. Figure 6 shows the average MAC error of all test cases for mass normalization, max. normalization and orthonormalization. Mass normalization is unfavorable, because it gives a higher L_2 norm to the higher frequency modes. Orthonormalization and max. normalization perform equally well and are therefore good choices for the POD algorithm.

Finally, the POD truncation level has to be selected. Commonly this is done by establishing the cumulative relative information content based on the POD eigenvalues. However, for the test case scenario the threshold selection was made based on the average error estimators. Figure 7

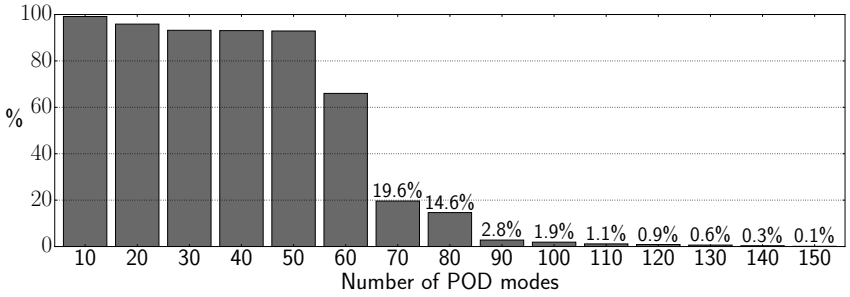

Figure 7: MAC error criterion for different truncation levels

shows the average MAC error for different truncation levels. No frequency limit to the POD snapshots is imposed, the first 150 modes are always considered. To reduce the MAC error below the best-practice threshold of 1%, 130 POD modes have to be retained. However, the choice was made to retain 150 modes, which is the same amount as the other reference selection method. This enables a clear performance comparison for the same computational cost.

4.2 Results

The flutter results of both test cases are presented in Figure 8. The presented modes are selected based on the largest observed deviations either in frequency or damping. A selection of frequency and damping curves for the nominal structure flutter computation is shown in Figure 8(a). The direct aerodynamics are used as verification result. Mode *A* and *D* show small deviations in the damping with the POD reference basis and modes *B* and *C* show small deviations with the nominal reference basis. However, overall the approximation with both reference selections is in excellent agreement with the direct aerodynamics reference solution. Thus, both methods could be used satisfactorily for flutter computations without structural deficiencies.

Figure 8(b) shows the frequency and damping progression for the failure case. As already shown in the error estimation study, the nominal reference selection method creates large deviations in both frequency and damping. On the other hand, the results of the POD reference set are in excellent agreement with the direct aerodynamics. The extra modal information on the failure case, which was part of the snapshot matrix in the POD input, is well represented in the reference basis and, thus, the approximation error is eliminated. The MAC error for the nominal reference and the POD-based reference for this computation are 8.5% and 0.1%, respectively. This is in good agreement with the frequency and damping results.

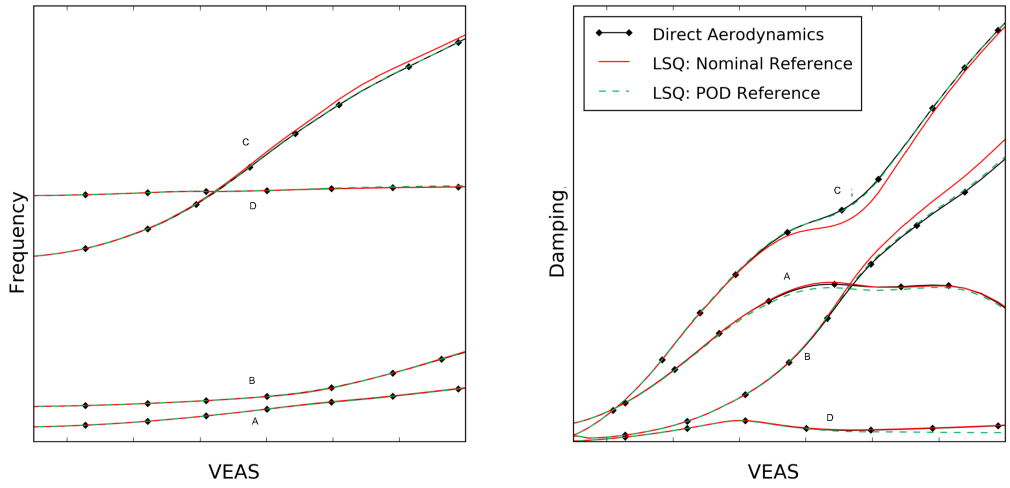

(a) Frequency and damping progression for the nominal structure flutter computation

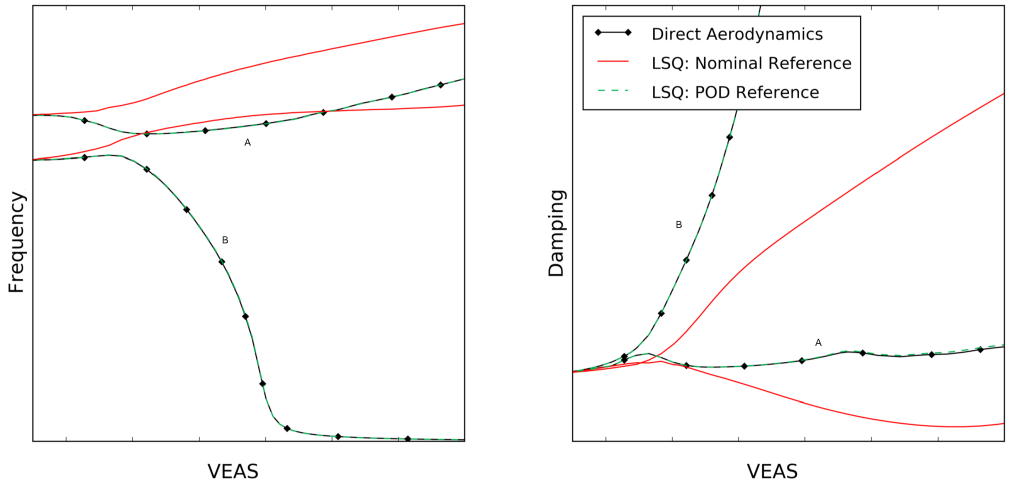

(b) Frequency and damping progression for the failure case

Figure 8: Comparison of flutter results for two test cases

5 CONCLUSION AND OUTLOOK

In this work, three different error estimators are compared to indicate the accuracy of a least-square approach approximating the aerodynamic force matrices. The criteria are used to judge if the given reference mode set can be used to accurately predict a flutter boundary or if the basis needs further enrichment. The modal assurance criterion was benchmarked against a local criterion based on the aerodynamically-weighted maximal displacements and a relative error in the diagonal elements of the aerodynamic force matrix for a discrete structural failure case of a transport aircraft. All three estimators performed equally well and therefore the simplest solution, the modal assurance criterion, was picked with a strict threshold of 1%. Note, if the criterion is fulfilled, the flutter results are reliable. However, exceeding the threshold not-necessarily results in inaccurate flutter boundaries, since the imprecisely captured modes might not participate in the dominating coupling mechanism. Nevertheless, if the error is too high, the reference mode set must be enriched. In the studied cases, a sufficient approximation is yielded adding the mode with the highest error. More sophisticated methods like extracting the most dominant error mode applying a proper orthogonal decomposition were not necessary.

Subsequently, the selection of a more robust set of reference modes for the least-square approach is analyzed. A basis consisting of modes from a nominal structural layout is compared to a basis obtained by a proper orthogonal decomposition comprising modes from nominal cases as well as failure cases. The total amount of reference modes considered within the least-square approximation is kept constant between both methods. Both sets perform equally well on nominal structural cases, whereas the reference basis containing only modes of a nominal structure exceeds the threshold for the modal assurance criterion considering the failure case. Contrary, the optimized set using proper orthogonal decomposition agrees excellently with the flutter reference solution using direct aerodynamics.

The new selection of the least-square reference set combined with the error estimator results in a robust process to approximate aerodynamic forces of different mass cases and structural layouts. Nevertheless, further improvements can be discussed, e.g. an automatic selection of the input modes for the single-value decomposition. Furthermore, the finite-element nodes used in the least-square approach are selected manually based on engineering experience. An automatic way by introducing a weighting of the nodes could be analyzed.

ACKNOWLEDGEMENT

The research leading to this work was part of a master thesis project conducted at Delft University of Technology in collaboration with Airbus GmbH. The authors wish to thank Dr. Ir. van Zuijlen of the Delft University of Technology for the valuable discussions and his support.

6 REFERENCES

[1] Thormann, R. and Widhalm, M. (2013). Linear-Frequency-Domain Predictions of Dynamic-Response Data for Viscous Transonic Flows. *AIAA Journal*, 51(11).

[2] Kreiselmaier, E. and Laschka, B. (2000). Small Disturbance Euler Equations: Efficient and Accurate Tool for Unsteady Load Prediction. *Journal of Aircraft*, 37(5).

[3] Pechloff, A. and Laschka, B. (2006). Small Disturbance Navier-Stokes Method: Efficient Tool for Predicting Unsteady Air Loads. *Journal of Aircraft*, 43(1).

[4] Stickan, B., Schröder, F., Helm, S., et al. (2018). On recent advances in industrial high-fidelity aeroelasticity. In R. Heinrich (Ed.), *AeroStruct: Enable and Learn how to Integrate Flexibility in Design*, Notes on Numerical Fluid Mechanics and Multidisciplinary Design. Springer Berlin Heidelberg.

[5] Allemang, R. J. (2003). The Modal Assurance Criterion - Twenty Years of Use and Abuse. *Sound and Vibration*, 14–20.

[6] Pastor, M., Binda, M., and Harcarik, T. (2012). Modal assurance criterion. *Procedia Engineering*, 48, 543–548.

[7] Taira, K., Brunton, S. L., Dawson, S. T. M., et al. (2017). Modal Analysis of Fluid Flows: An Overview. *AIAA Journal*, 55(12).

[8] Lumley, J. L. (1967). The Structure of Inhomogeneous Turbulent Flows. In A. M. Yaglam and T. V. I. (Eds.), *Proceedings of the International Colloquium on the Fine Scale Structure of the Atmosphere and Its Influence on Radio Wave Propagation*. Nauka, Moscow: Doklady Akademii Nauk SSSR.

[9] Berkooz, G., Holmes, P., and Lumley, J. L. (1993). The proper orthogonal decomposition in the analysis of turbulent flows. *Annual Review of Fluid Mechanics*, 25, 539–575.

[10] Bekemeyer, P., Thormann, R., and Timme, S. (2017). Rapid gust response simulation of large civil aircraft using computational fluid dynamics. *The Aeronautical Journal*, 121(1246), 1795–1807.

[11] Bekemeyer, P. and Timme, S. (2017). Reduced Order Transonic Aeroelastic Gust Response Simulation of Large Aircraft. In *35th AIAA Applied Aerodynamics Conference*. Denver, Colorado: AIAA Paper.

[12] Hall, K. C., Thomas, J. P., and Dowell, E. H. (2000). Proper Orthogonal Decomposition Technique for Transonic Unsteady Aerodynamic Flows. *AIAA Journal*, 38(10), 1853–1862.

[13] Wright, J. R. and Cooper, J. E. (2014). *Introduction to Aircraft Aeroelasticity and Loads*. John Wiley & Sons, Ltd., 2nd ed.

[14] MSC-Software (2018). MSC-Nastran. `http://www.mscsoftware.com`. [Online; accessed 2018-12-14].

[15] Schwamborn, D., Gerhold, T., and Heinrich, R. (2006). The DLR TAU-code: Recent applications in research and industry. In *European Conference on Computational Fluid Dynamics*. Egmond aan Zee, The Netherlands: ECCOMAS CFD.

[16] Meinel, M. and Einarsson, G. (2010). The FlowSimulator framework for massively parallel CFD applications. *PARA 2010: State of the Art in Scientific and Parallel Computing*.

[17] Stickan, B., Bleecke, H., and Schulze, S. (2013). Nastran based static cfd-csm coupling in flowsimulator. In N. Kroll, R. Radespiel, J. W. Burg, and K. Srensen (Eds.), *Computational Flight Testing*, vol. 123 of *Notes on Numerical Fluid Mechanics and Multidisciplinary Design*. Springer Berlin Heidelberg. ISBN 978-3-642-38876-7, pp. 223–234.

[18] Stickan, B. (2018). *Explanation of AEROSTABIL Limit-Cycle Oscillations via High-Fidelity Aeroelastic Simulations*. Deutches Zentrum für Luft- und Raumfahrt, Institut für Aeroelastik. ISBN 1434-8454.

[19] Kaiser, C., Thormann, R., Dimitrov, D., et al. (2015). Time-Linearized Analysis of Motion-Induced and Gust-Induced Airloads with the DLR TAU Code. In *64th Deutscher Luft- und Raumfahrtkongress*. Rostock, Germany: Deutsche Gesellschaft für Luft- und Raumfahrt. ISBN 370189, pp. 1–9.

[20] Spalart, P. R. and Allmaras, S. R. (1992). A One-Equation Turbulence Model for Aerodynamic Flows. In *30th Aerospace Sciences Meeting & Exhibit*. Boeing Commercial Airplane Group, Reno, NV: AIAA.

COPYRIGHT STATEMENT